

Rapid Increase in Plasma Membrane Chloride Permeability during Wound Resealing in Starfish Oocytes

Alan Fein and Mark Terasaki

Department of Cell Biology, University of Connecticut Health Center, Farmington, CT 06030

Plasma membrane wound repair is an important but poorly understood process. We used femtosecond pulses from a Ti-Sapphire laser to make multiphoton excitation-induced disruptions of the plasma membrane while monitoring the membrane potential and resistance. We observed two types of wounds that depolarized the plasma membrane. At threshold light levels, the membrane potential and resistance returned to prewound values within seconds; these wounds were not easily observed by light microscopy and resealed in the absence of extracellular Ca^{2+} . Higher light intensities create wounds that are easily visible by light microscopy and require extracellular Ca^{2+} to reseat. Within a few seconds the membrane resistance is ~ 100 -fold lower, while the membrane potential has depolarized from -80 to -30 mV and is now sensitive to the Cl^- concentration but not to that of Na^+ , K^+ , or H^+ . We suggest that the chloride sensitivity of the membrane potential, after wound resealing, is due to the fusion of chloride-permeable intracellular membranes with the plasma membrane.

INTRODUCTION

The permeability barrier of the cell, which is the lipid bilayer of the plasma membrane, is less than 10 nm thick. Mechanical forces can easily disrupt this boundary, but there are robust cellular mechanisms for repair. This has been demonstrated *in vitro* by experiments on cells in culture (McNeil et al., 1984). Mechanical trauma produces wounds that are sealed *in vivo* during eccentric exercise in muscle or at regions of turbulent flow in arteries (McNeil and Khakee, 1992; Yu and McNeil, 1992), indicating that plasma membrane wounding and repair is likely to be an important process in pathophysiology.

88 years ago, experimental studies of wound repair were begun by Chambers, who showed remarkable healing of gross wounds in echinoderm eggs made by glass needles (Chambers, 1917). Heilbrunn showed that healing of such wounds requires extracellular calcium in the millimolar range (Heilbrunn, 1930). Recent experimental studies of wound healing have been conducted on several different systems using a variety of methods for producing disruptions. These studies have shown that the time required for sealing, the involvement of intracellular organelles, and the requirement for calcium vary according to cell type and the means by which the disruptions are made (for review see McNeil and Steinhardt, 2003).

Small wounds made by electroporation reseat without requirement for extracellular Ca^{2+} . Electroporation-induced wounds in red blood cells seal within a few seconds and clearly do so without the presence of intracellular membranes (Chang and Reese, 1990), and in

sea urchin eggs electroporation-induced wounds reseat in much less than a second (Hibino et al., 1993).

Other wounds, generally thought to be larger than the electroporation-induced wounds, seem to involve the exocytosis of intracellular organelles and require calcium. For example, wounding of cultured mammalian cells by microneedles has been extensively studied. Repair occurs in 10–30 s, requires extracellular calcium, and fusion of intracellular organelles with the plasma membrane (exocytosis) is required (Steinhardt et al., 1994), probably accounting for the calcium involvement. The identity of the organelles required for membrane resealing remains unresolved (Reddy et al., 2001; Cerny et al., 2004; Shen et al., 2005) as does the specific identity of the molecules involved in the fusion process (Detrait et al., 2000b; Reddy et al., 2001; Bansal et al., 2003; Shen et al., 2005).

As another example, when large diameter axons of various invertebrates are transected, the cut end reseals completely only after about an hour. The evidence suggests that vesicles formed by endocytosis migrate to the transection site where they form a tight plug, first without any membrane fusion, but eventually fusing together and with the axonal membrane to form the final seal (Spira et al., 1993; Eddleman et al., 2000). As with mammalian cells, progress has been made in identifying the molecules that are involved in axon repair (Detrait et al., 2000a).

Lastly, large plasma membrane disruptions, of the type originally made by Chambers and Heilbrunn, have

Correspondence to Alan Fein: afein@neuron.uconn.edu

Abbreviations used in this paper: ASW, artificial seawater; CFSW, calcium-free seawater; NSW, natural seawater.

been made in echinoderm eggs by ripping off large fragments of membrane (Terasaki et al., 1997) or by local application of the detergent Triton X-100 (McNeil et al., 2000). Under these conditions, repair requires calcium and seems to occur within a few seconds through a calcium-dependent fusion of yolk platelets to each other and to the plasma membrane (for review see McNeil and Steinhardt, 2003). The yolk platelets are likely to be derived from endocytic membranes during oocyte development, as they are in other species such as frog (Opresko et al., 1980).

One approach that has not been exploited with oocytes is to monitor the plasma membrane by electrophysiological methods while it is undergoing disruption and repair. The experimental difficulty is that mechanical methods of wounding can disrupt the seal around the electrode, causing electrical artifacts. This can be circumvented by using femtosecond pulses from a Ti:Sapphire laser to make multiphoton excitation-induced disruptions of the plasma membrane (Galbraith and Terasaki, 2003). We have undertaken a combined electrophysiological and optical study of membrane disruption and repair using oocytes from the starfish *Asterina miniata*. These cells are well suited for electrophysiology due to their uniform size, and to their spherical geometry and low cytoplasmic resistance, which makes them easy to voltage clamp (Hagiwara et al., 1975).

MATERIALS AND METHODS

Pacific coast bat stars (*Asterina miniata*) were collected at either the Bodega Marine Lab or by Marinus and were maintained in a seawater tank. To obtain oocytes, a small piece of ovary was removed through a hole cut in the skin; the ovary was minced in 15 ml room temperature calcium-free sea water, agitated to release oocytes, and then after ~1 min, the ovary clumps were removed and discarded. The oocytes were monitored by light microscopy until most of the follicle cells were detached (<5 min) at which point 0.15 ml 1 M CaCl₂ was added to restore normal calcium. After settling, the oocytes were transferred to natural seawater and kept at 16–20°C. Fully grown immature oocytes (170–180 μm diameters) were used for experiments, which were done at room temperature (20°C). For some experiments, the vitelline envelope was removed by incubating oocytes for 30 min at room temperature in 100 μg/ml Type XIV protease (P5147; Sigma-Aldrich).

We used a Carl Zeiss MicroImaging, Inc. LSM 510 NLO system on an inverted Axiovert 200 microscope. It was equipped with a Mira Ti:Sapphire laser pumped by an 8W Verdi pump laser (Coherent). The microscope was focused at the equator of the oocyte (i.e., 80–90 μm from the coverslip) using a Carl Zeiss MicroImaging, Inc. 25× multi-immersion plan-neofluar (N.A. 0.8) objective lens. The laser spot was scanned once in a line of length ~10 μm, intersecting perpendicularly with the cell surface. At full laser power tuned at 800 nm, the energy at the focal plane was ~100 mW, and when scanned at the slowest speed (205 μs/pixel), this invariably caused a large wound such as shown in Fig. 1 A. To make small wounds as exemplified in Fig. 1 B, we started with a low, nonwounding intensity at a faster scan speed (e.g., 25 μs/pixel). The laser intensity was increased in increments of 1%

until the intensity was reached at which a wound occurred (as signaled by a membrane depolarization at the time of the line scan); if no wound occurred at full laser power, we decreased the scan speed and repeated the process.

To monitor permeability to small molecules following wounding, oocytes were suspended in 0.5 mg/ml calcein (MW = 623) in sea water. The bleach program of the LSM 510 microscope software was used in which the bleach region was a line scan across the surface. Because the scanning rate cannot be changed during the experiment, a fast scan rate was used to collect images rapidly; with the fast rate, it was necessary to use multiple line scans (20–400) to make the wound. The LSM 510 produces a sync pulse at the beginning and end of the bleach period; this was used to synchronize the simultaneous optical and electrophysiological recordings. We only recorded electrical responses when the laser beam was positioned to wound the plasma membrane and not when the wounding beam was positioned in the cytoplasm or the extracellular space.

For single electrode experiments, a modified version of a microinjection chamber (Terasaki and Jaffe, 1993) allowed manipulation of the electrode in the plane of focus using a Narishige SM-20 micromanipulator. For voltage clamp experiments, which required two electrodes with access from above, we used an open chamber with a round coverslip bottom (25 mm; Fisher Scientific). A nylon mesh with 149 μm opening (Small Parts) was tacked down to the coverslip with silicon grease. Oocytes in a small drop of seawater were drawn by surface tension into the mesh openings, after which the chamber was filled with seawater.

Oocytes were impaled with either one or two single-barreled microelectrodes, which were formed on a P-97, Flaming/Brown micropipette puller (Sutter Instrument Co.). Electrodes were filled with 2M KCl and had a resistance of around 10 MΩ. An Axoclamp-2B current and voltage clamp amplifier (Axon Instruments) was used for current clamp recording of membrane potential or for recording membrane current when performing a two electrode voltage clamp. During current clamp recordings, membrane resistance was monitored by passing 1 nA of hyperpolarizing inward current through the membrane via the intracellular pipette. The voltage drop across the pipette resistance, resulting from the 1 nA current pulse, was balanced out using the amplifier's bridge balance. PClamp 9 was used to record experimental data by computer (Axon Instruments). Data from pClamp was output to Origin 7.5 (Microcal Software) and Coreldraw 12.0 (Corel Corp.) for preparation of figures. Unless otherwise specified, results were repeated in at least 10 cells, and when analyzed statistically, results are given as the mean ± SD.

Natural seawater (NSW) was obtained from the supply department of the Marine Biological Laboratory. Artificial seawater (ASW) was, in mM, 483 NaCl, 10 KCl, 11 CaCl₂, 29 MgSO₄, 27 MgCl₂, 2.4 NaHCO₃, pH 8.0. For calcium-free seawater (CFSW), NaCl replaced CaCl₂, and for choline ASW, choline Cl replaced NaCl. For pH 7.0 ASW, 10 mM Hepes replaced NaHCO₃ and the pH was set at 7.0. For 100 mM K⁺ ASW, NaCl was reduced to 393 mM and KCl increased to 100 mM. For Na isethionate ASW, NaCl was replaced by Na isethionate. ASW was mixed with Na isethionate ASW to make solutions having chloride concentrations in between that of ASW and Na isethionate ASW. Omitting MgCl₂ from Na isethionate ASW made ASW with 32 mM Cl⁻. For low calcium experiments, a stock solution of 500 mM EGTA, pH 8.0, was used to make 1 mM EGTA in CFSW. To transfer the oocytes to this solution, 5 μl of oocytes in ASW were added to 2 ml of EGTA-buffered CFSW in a test tube; after settling, oocytes were transferred to the observation chamber, which was filled with additional EGTA-buffered CFSW.

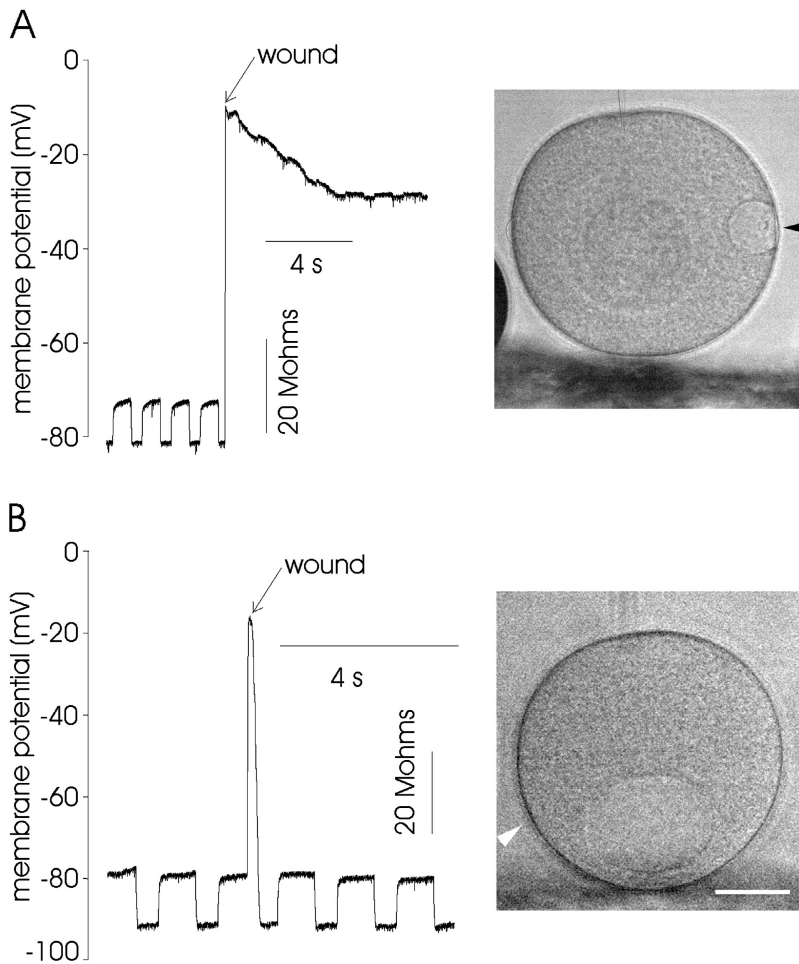


Figure 1. Two distinct types of changes in membrane potential and membrane resistance caused by wounding the plasma membrane of starfish oocytes. (A) Wounding with a high light intensity causes a sustained change in the membrane potential. In the photomicrograph, there is a large hemispherical indentation where the line scan occurred (black arrowhead). The wound appears similar to wounds produced by local application of Triton X-100 detergent to the surface of sea urchin eggs, where the hemispherical boundary was shown to be continuous with the plasma membrane (McNeil et al., 2000). (B) Wounding with threshold light intensities causes a rapid depolarization of the plasma membrane, which rapidly returns to its value before wounding. In the photomicrograph there is no discernible effect of the wounding on the cell membrane in the region where it was wounded (white arrowhead). The $\sim 50 \mu\text{m}$ spherical structure inside the oocyte is the nucleus. In the records of A and B, the membrane resistance was monitored by measuring the change in membrane potential resulting from a repeated 1-nA current pulse delivered to the cell via the intracellular pipette. See text and MATERIALS AND METHODS for further experimental details. Bar, $50 \mu\text{m}$.

RESULTS

Two Types of Wounds

Oocytes were bathed in NSW and impaled with a single microelectrode used to monitor the membrane potential and membrane resistance under current clamp (see MATERIALS AND METHODS). To make a disruption, the diffraction-limited laser spot of the scanning microscope was made to scan a single line perpendicular to the cell surface. High laser intensities always caused a hemispherical depression in the cell surface visible at low power magnification (Fig. 1 A); this resembles the wound made by local application of Triton X-100 (McNeil et al., 2000). Electrically, this type of wound was characterized by a rapid membrane depolarization of $\sim 60 \text{ mV}$ after which the membrane potential, over several seconds, approached a value of about -30 mV . Additionally, the membrane resistance following the wound dramatically decreased to a value below what could be measured reliably by the bridge amplifier. The membrane slope resistance with the membrane potential voltage clamped at -30 mV decreased ~ 100 -fold after wounding to the range of $100 \text{ k}\Omega$ to $1 \text{ M}\Omega$ (unpublished data).

We also observed a transient response as shown for the cell in Fig. 1 B. The wound was characterized by a brief membrane depolarization of $\sim 60 \text{ mV}$, and the membrane potential and resistance after the wound were approximately the same as before wounding. Furthermore, the photomicrograph in Fig. 1 B shows no obvious residual membrane damage in the region of the cell where the line scan of threshold light intensity occurred. At this magnification, it would not have been apparent that a wound had occurred, without electrical recording of membrane potential (however see Figs. 4 and 7). By starting with a low, nonwounding laser intensity then increasing the laser power in 1% increments, we were able to produce the transient response of Fig. 1 B. However, even with this threshold protocol, many oocytes only gave the response shown in Fig. 1 A, indicating that the energy range for causing the transient response is relatively narrow. First we will consider wounds of the type caused by high laser intensities, afterward we will consider the wounds produced by threshold light intensities.

Wounds Caused by High Laser Intensities

As mentioned in INTRODUCTION, extracellular calcium is required to repair large wounds similar to that

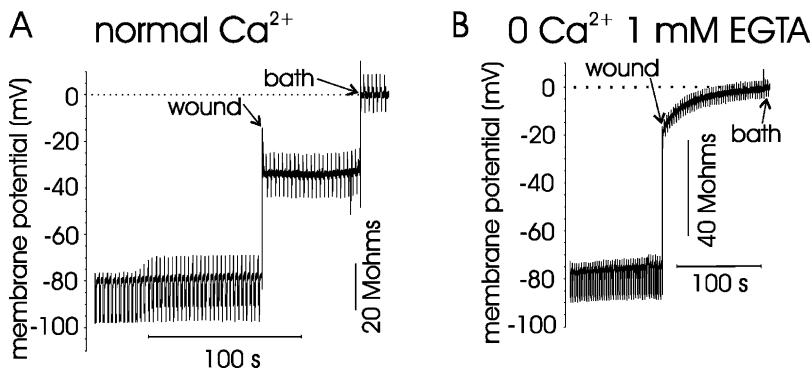


Figure 2. The effect of extracellular calcium on the electrical response to wounding. (A) After wounding, the oocyte in normal Ca^{2+} ASW, the membrane potential is approximately -30 mV, and the membrane resistance is below the resolution of the bridge monitor. (B) After wounding the oocyte in 0 Ca^{2+} 1 mM EGTA ASW, the membrane potential slowly goes to approximately zero and the membrane resistance is below the resolution of the bridge monitor. At the end of each experiment in A and B, the intracellular pipette was withdrawn from the cell into the bath to confirm the value of the membrane potential. See text for further experimental details.

in Fig. 1 A. Accordingly, we compared the wound response in the presence or absence of extracellular Ca^{2+} (Fig. 2). For 10 cells, the membrane potential, after wounding in NSW, was -29.5 ± 2.5 mV. Following wounding of cells bathed in 0 Ca^{2+} 1 mM EGTA ASW, the membrane potential goes toward 0 mV and the membrane resistance is below the resolution of the bridge amplifier (Fig. 2 B). For 13 cells, the membrane potential, after wounding in 0 Ca^{2+} 1 mM EGTA ASW, was -1.4 ± 0.52 mV. These findings are in agreement with the earlier work that extracellular Ca^{2+} is required for wound healing to occur.

Several possible repair mechanisms might account for the depolarization of the plasma membrane during recovery from wounding (Fig. 1 A). One possibility is that membrane vesicles may have accumulated at the wound site, forming a low resistance membrane plug, as has been proposed to occur at the ends of cut axons (Spira et al., 1993; Eddleman et al., 2000). Another possibility is that the plasma membrane has been sealed by fusion of intracellular membranes, and the depolarization results from a change in the ionic permeability of the plasma membrane. To distinguish between these possibilities, we performed ion substitution experiments since a membrane plug would not be expected to exhibit ionic selectivity. Substituting choline for sodium, decreasing the pH to 7.0, or increasing K^+ from 10 to 100 mM in the solution bathing the cells, had no significant effect (Student's *t* test, $P < 0.01$) on the membrane potential following wounding (Fig. 3 B). In contrast, replacing 483 mM NaCl with Na isethionate resulted in a $+5$ mV membrane potential after wounding (Fig. 3, A and B), indicating high Cl^- permeability of the plasma membrane. To further characterize the Cl^- permeability of the plasma membrane, for these wounds, we wounded cells bathed in solutions with different Cl^- concentrations. The data for the membrane potential after wounding (Fig. 3 C) is fit by a straight line with a slope of -33.2 mV per decade for Cl^- . This is well below the ideal slope of -58 mV per decade for a membrane perfectly selective to Cl^- .

It takes several seconds for the membrane potential to reach a plateau following wounding: 4.3 ± 1.3 s ($n = 11$) in 569 mM Cl^- and 8.8 ± 3.7 s ($n = 9$) in 86 mM Cl^- . However, the data in Fig. 1 A and Fig. 3 A suggest that the plasma membrane exhibits Cl^- permeability well before the membrane potential reaches a plateau. This can be seen in Fig. 3 D where we have superimposed the recordings from Fig. 1 A and Fig. 3 A, by aligning them at the moment of wounding. As early as 1 s after wounding, the membrane potentials can be seen to move in opposite directions toward their respective plateau values. This suggests that the plasma membrane is starting to exhibit chloride permeability as early as 1 s following wounding.

We monitored wound healing in a different way by imaging cells in the presence of a fluorescent probe in the sea water. Cells were bathed in a saturated solution of calcein, a bright fluorescein analogue (623 D) that is impermeant to membranes, and were impaled with an electrode in order to simultaneously monitor membrane potential and membrane resistance. The Ti-Sapphire laser was used to wound and to image; a slightly different scanning procedure was used in order to obtain images rapidly after wounding (see MATERIALS AND METHODS). As expected, when cells were bathed in calcium-free sea water (0 Ca^{2+} added, 1 mM EGTA), calcein entered the wound site and diffused throughout the cytoplasm (unpublished data, $n = 5$ cells). In sea water, calcein began to enter but was stopped at the boundary of the hemispherical depression previously seen by transmitted light (Fig. 4). Although it takes a few seconds for calcein to completely fill the depression, the movement of calcein in a direction parallel to the plasma membrane along the sides of the depression is blocked as early as 1 s. This suggests that internal membranes had already fused with the plasma membrane at the edge of the wound by that time.

The oocyte surface is associated with an extracellular matrix called the vitelline envelope. Examination of the wound site indicated that extracellular debris was trapped between the plasma membrane and the vi-

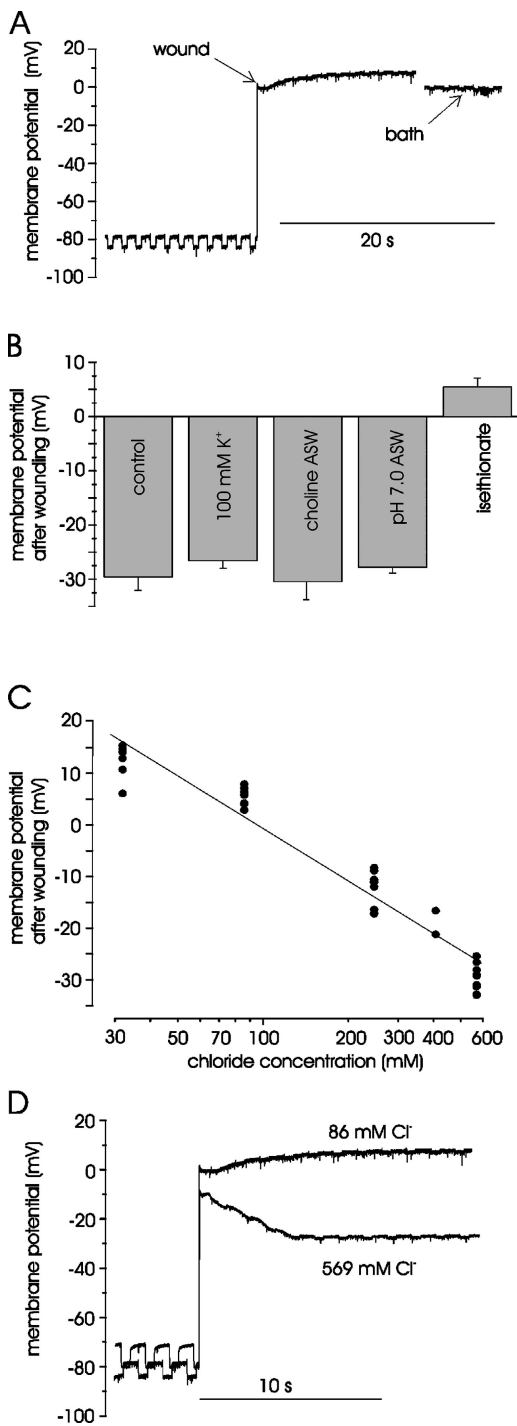


Figure 3. Chloride ion permeability contributes to the membrane potential following wounding. (A) The cell was bathed in Na isethionate ASW and subsequently wounded. At the end of the experiment, the intracellular pipette was withdrawn from the cell into the bath to confirm the value of the membrane potential. (B) Effect of ion substitution on the membrane potential (mean \pm SD) following wounding. Control, ASW ($n = 10$), 100 mM K^+ ASW ($n = 6$), choline ASW ($n = 7$), pH 7.0 ASW ($n = 6$), Na isethionate ASW ($n = 9$). (C) Cl^- dependence of the membrane potential after wounding. The data were fit with a straight line solely for the purpose of providing a quantitative estimate of the chloride dependence of the membrane potential after wounding.

telline envelope. It occurred to us that the contents of the yolk platelets that were exocytosed during resealing may get trapped by the vitelline envelope and may force the resealed surface to have the shape of a concave depression. To test this idea, the vitelline envelope was removed by protease treatment (see MATERIALS AND METHODS); cell wounding resulted in an outward bulging region rather than a hemispherical depression, and very little calcein appeared to enter the cell (Fig. 5; $n = 7$ cells).

Wounds Caused by Threshold Laser Intensities

When we used threshold light intensities, we discovered that the cell's response to wounding, in the absence of extracellular Ca^{2+} , was the same as in normal Ca^{2+} . Fig. 6 A shows the response of a cell bathed in 0 Ca^{2+} 1 mM EGTA ASW to wounding. The wound resulted in a transient membrane depolarization of ~ 60 mV, and the membrane resistance after the wound was approximately the same as before wounding. Moreover, at this magnification, there was no obvious residual membrane damage in the region of the cell where the line scan occurred (unpublished data). This indicates that wounds caused by threshold light intensities do not require the presence of extracellular Ca^{2+} in order to heal. To estimate the size of these wounds, we recorded from oocytes held under voltage clamp (Fig. 6 B). Cells were bathed in 0 Ca^{2+} 1 mM EGTA ASW and impaled with two microelectrodes and voltage clamped at -30 mV. The membrane potential was repeatedly ramped from -35 to -25 mV in order to monitor the slope resistance of the plasma membrane at -30 mV (Fig. 6 B, top). As can be seen in the lower current trace of Fig. 6 B, membrane disruption resulted in an inward current of ~ 6 nA in magnitude. In addition, there was no change in the membrane currents evoked by the voltage ramps as a result of wounding, indicating that there was no significant change in the slope resistance of the membrane. For eight cells, the magnitude of the peak inward current measured in 0 Ca^{2+} 1 mM EGTA ASW was 4.5 ± 3.5 nA. Assuming the wound forms a 10-nm-long cylinder through the lipid bilayer, filled with CFSW, the diameter of the cylinder would need to be ~ 40 nm to produce a current of 4.5 nA. Remember from Fig. 1 B that this type of wound is also seen in the presence of calcium in the NSW. The magnitude of the peak inward current of these wounds

(D) Superimposition of the recordings of Fig. 1 A and Fig. 3 A aligned at the time of wounding. For oocytes bathed in 100 mM K^+ , the resting membrane potential before wounding was -21.1 ± 1.4 mV ($n = 6$ cells) because the plasma membrane of mature and immature starfish oocytes exhibit an inwardly rectifying K^+ current that predominately sets the resting membrane potential (for example see Shen and Steinhardt, 1976).

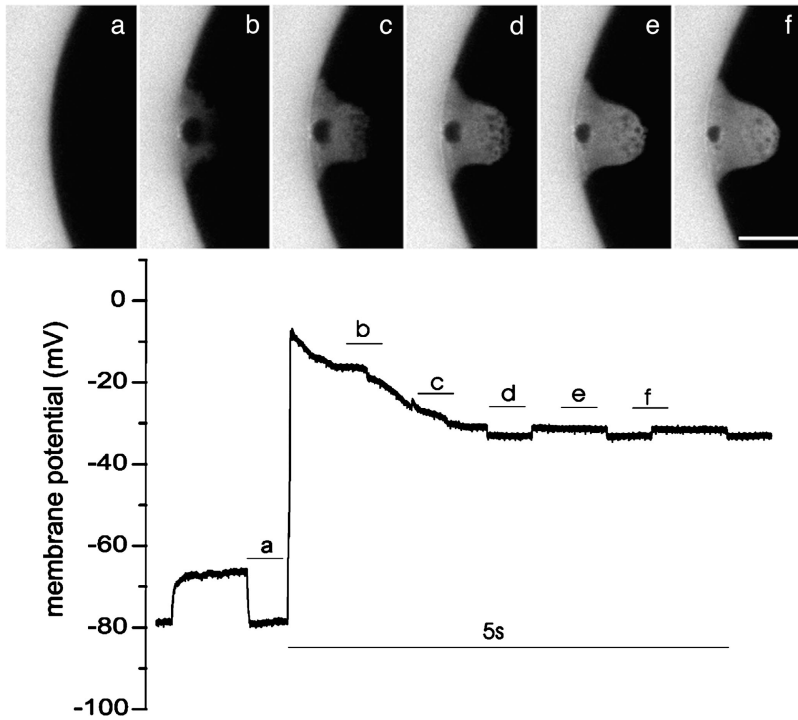


Figure 4. Simultaneous electrical recording and fluorescence imaging during wound resealing. Oocytes were immersed in calcein-containing sea water and imaged before and after plasma membrane disruption while the membrane potential and membrane resistance of the oocyte were monitored simultaneously. Each image was obtained at the corresponding times indicated on the electrical recordings below. The dark spot at the wound site, which shrinks over time, and is just below where the membrane was, is a gas bubble that sometimes forms after wounding. Bar, 50 μm .

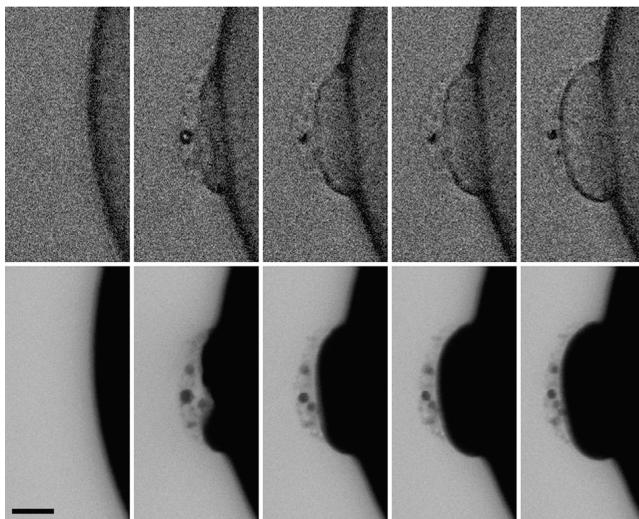


Figure 5. Effect, on wound healing, of removing the oocyte extracellular matrix. The vitelline envelope was removed by protease treatment (see MATERIALS AND METHODS). The oocyte was immersed in sea water containing 0.5 mg/ml calcein and wounded using the same wounding protocol as in Fig. 4. Fluorescence (bottom) and transmitted light (top) images were obtained simultaneously. The first time point shown was taken just before the wound. The second time point shown is the first image taken after the wound, and the other time points are the successive images taken at 0.985-s intervals. In contrast to Fig. 1 A, where the vitelline envelope was present, the cytoplasm bulges outward. Very little calcein appears to enter the cell. Extracellular debris can be seen, particularly as negative fluorescence images; this debris may arise from the yolk granule contents released into the sea water after fusion with the plasma membrane. Bar, 10 μm .

measured under voltage clamp in NSW was (154 ± 90 nA, $n = 10$). The diameter of the wound in NSW would need to be $\sim 1.0 \mu\text{m}$ to sustain the larger current.

Threshold wounds were made with calcein present in the bathing solution in order to image extracellular fluorescent dye entry during disruption and sealing. For cells bathed in NSW, we found (unpublished data, $n = 13$ cells) that a small concave membrane depression forms at the wound site during healing. When we repeated the same experiment for cells bathed in 0 Ca^{2+} 1 mM EGTA ASW, we also observed the formation of a small concave depression (Fig. 7) at the wound site for 6 of 14 cells. For the other eight cells, there was no obvious change in calcein fluorescence in the vicinity of the region wounded.

DISCUSSION

By using a multiphoton scanning microscope to make wounds in the cell surface, we have been able to make electrical measurements during wound disruption and repair as well as near-simultaneous imaging of permeability to extracellular fluorescent probes. In the experimental system that we used, echinoderm eggs, there is considerable evidence that extracellular Ca^{2+} entering the cell through a plasma membrane disruption triggers fusion of yolk platelets to repair the wound (McNeil et al., 2000; McNeil and Steinhardt, 2003). We now provide data on the speed with which repair occurs and on resultant changes in plasma membrane ionic permeability.

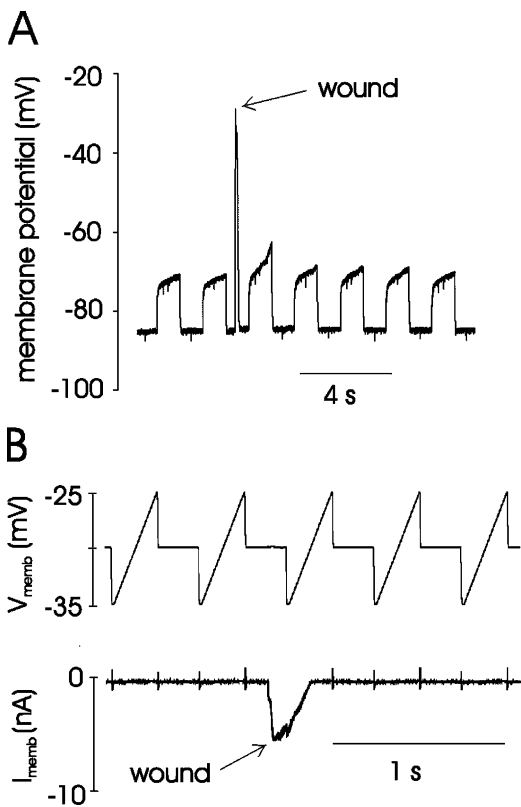


Figure 6. Extracellular calcium is not required for recovery from wounds caused by threshold light intensities. (A) A threshold light causes a rapid depolarization of the plasma membrane, which rapidly returns to its value before wounding. Similarly the membrane resistance after wounding is approximately the same as it was before the wound. (B) Membrane current measured under voltage clamp during wounding resulting from threshold intensity multiphoton excitation. The cell was impaled with two microelectrodes and placed under voltage clamp at a holding potential of -30 mV. The membrane potential was repeatedly ramped from -35 to -25 mV in order to monitor the slope resistance of the plasma membrane around -30 mV, see upper membrane potential trace. Wounding the cell caused a transient inward current having peak amplitude of ~ 6 nA (see lower membrane current trace). The cells in A and B were bathed in 0 Ca^{2+} 1 mM EGTA ASW throughout the experiment. See text for further experimental details. We follow the convention of showing inward currents as a downward deflection.

Wounds Caused by High Laser Intensities

Within a few seconds of a laser-induced disruption, the membrane potential stabilizes at -30 mV (Fig. 1 A), and a barrier to extracellular fluorescent dye entry is established (Fig. 4). For oocytes with the vitelline envelope removed, we were unable to detect calcein entry into the original confines of the cell as early as 0.985 s after wounding (Fig. 5). This time course is significantly faster than the 10 – 30 s required for sealing in cultured mammalian cells. Echinoderm eggs are normally shed and fertilized in the open ocean, so perhaps they have evolved an unusually efficient membrane repair capability to survive in that hazardous environment.

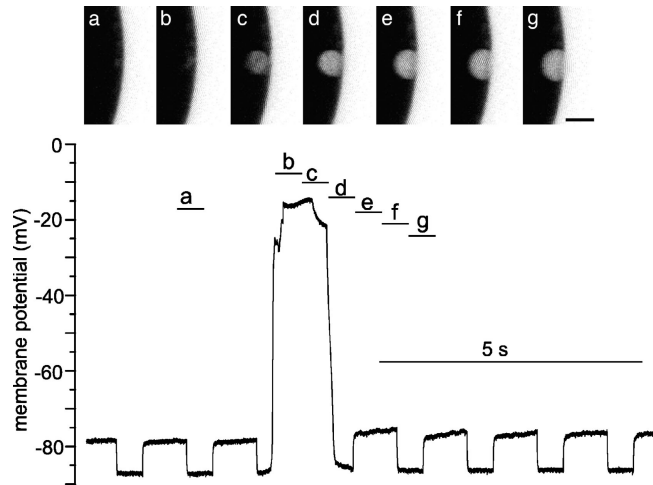


Figure 7. Simultaneous electrical recording and fluorescence imaging during wound resealing in calcium-free sea water. Oocytes were immersed in calcein-containing CFSW and imaged before and after plasma membrane disruption while the membrane potential and membrane resistance of the oocyte were monitored simultaneously. Each image was obtained at the corresponding times indicated on the electrical recordings below. Bar, 10 μm .

After the wound is resealed, the plasma membrane resistance has decreased ~ 100 -fold and the membrane is highly permeable to Cl^- . Two possibilities might explain how the plasma membrane became permeable to Cl^- . First, the molecules responsible for the Cl^- permeability may have been present in the plasma membrane before wounding but with the permeability inactivated so that their presence was undetectable before wounding. The plasma membrane of mature and immature starfish oocytes has been reported to exhibit an inwardly rectifying K^+ current and a regenerative action potential due to Na^+ and Ca^{2+} (for example see Shen and Steinhardt, 1976) with no evidence for a Cl^- permeability. If there is an inactivated Cl^- permeability in the plasma membrane, then the localized wound would have to generate some type of signal, other than membrane depolarization, to activate the permeability.

The second possibility is that the Cl^- permeability is present originally in the yolk platelets and inserted into the plasma membrane at the time of repair. The presence of Cl^- permeability in yolk platelets, an organelle that is likely to be derived from endocytic membranes, is consistent with a variety of evidence, indicating that endosomal organelles and lysosomes are Cl^- permeable (Gunther et al., 1998; Debska et al., 2001; Demarex, 2002; Nilius and Droogmans, 2003). Since the wound site comprises $<5\%$ of the total oocyte surface area, the Cl^- permeability would likely be present at a high density in order for it to dominate the membrane potential after insertion. The on cell patch clamp technique might be used to detect the Cl^- permeability if

the debris on the surface of the wounded membrane (Fig. 5) could somehow be removed.

If the Cl^- permeability is indeed localized to the wound site, then one would predict that there should be a positive injury current flowing into the cell (carried by Cl^- flowing out of the cell) at the site of injury. This hypothetical oocyte injury current would be analogous to injury currents that flow out of wounded regions of epithelium, and which are thought to play a role in healing the wounded epithelium (Nuccitelli, 2003). Likewise, the hypothetical injury current in the oocyte may play a role in the steps of healing the wound that follow the initial sealing of the hole by exocytosis.

Lastly, we observed large differences in the shape of the resealed plasma membrane surface after wounding, depending on whether the vitelline envelope extracellular matrix was present or not; it was concave in its presence but convex in its absence. It is possible that oocyte cytoplasm tends to flow outwards from regions where the actin cortex is damaged, and that this outwards flow is prevented by the presence of the vitelline envelope, which traps the yolk platelet contents released during resealing and causes the repaired region to take on a concave shape. The effect of the vitelline envelope suggests that other factors in addition to membrane fusion can have a large effect on the shape that the repaired region takes on.

Wounds Caused by Threshold Laser Intensities

The discussion so far pertains to wounds easily made using high laser intensities. There was a second type of wound response that could be produced intentionally by a threshold protocol, i.e., by starting with low non-wounding laser intensity and increasing the intensity in very small steps. Threshold wounds often failed to occur even with this protocol, and thus must occur within a small window of laser power, suggesting that this type of disruption might be equally difficult to produce in natural conditions or by other experimental methods.

The threshold wound response was characterized by a brief depolarization indicative of a disruption, followed by a return of the membrane potential to its pre-wound level. From the instantaneous peak current in NSW, the disruption diameter was estimated to be $\sim 1 \mu\text{m}$. The same type of response could be produced in the absence of extracellular Ca^{2+} . However, the instantaneous peak current was smaller; consistent with a wound diameter that was $\sim 25\times$ smaller, suggesting that the resealing process involved is somewhat more efficient in the presence of extracellular Ca^{2+} .

In the absence of extracellular Ca^{2+} , some of the threshold wounds sealed without any visible change in the surface by fluorescence microscopy with extracellular calcein (8 of 14 cells). This appears to be similar to

brief, transient disruptions induced by electroporation, where sealing does not require extracellular Ca^{2+} (Chang and Reese, 1990; Hibino et al., 1993), and which have been interpreted as spontaneous sealing of the plasma membrane without the involvement of internal membranes.

However, some threshold wounds in the absence of extracellular Ca^{2+} resulted in a small hemispherical depression visible by fluorescence microscopy with extracellular calcein (6 of 14 cells), which seems inconsistent with simple plasma membrane closure. We suggest that this results from the exocytosis of internal vesicles to the plasma membrane; this membrane fusion apparently does not require extracellular Ca^{2+} , perhaps there is some Ca^{2+} contribution resulting from laser-induced disruption of cortical granules, which contain a large amount of Ca^{2+} (Gillot et al., 1989).

Several possibilities could explain this finding. First, the amount of membrane added during threshold wound sealing does not add enough chloride permeability to change the membrane potential. Another possibility is that threshold wounds are resealed primarily using cortical granules while high intensity wounds use primarily yolk platelets. One would then have to suppose that cortical granules have a much lower Cl^- permeability than yolk platelets. A third possibility is that the Cl^- permeability is present in the plasma membrane before wounding but with the permeability inactivated and that the threshold wound does not produce a large enough signal to activate the permeability. This would imply that a $1\text{-}\mu\text{m}$ hole in the plasma membrane does not generate a large enough signal to activate the Cl^- permeability.

In summary, we have used electrophysiological and optical methods to demonstrate very robust plasma membrane repair mechanisms in the starfish oocyte. Large disruptions are sealed within a few seconds at most, possibly by Ca^{2+} -dependent fusion of chloride-permeable intracellular organelles with the plasma membrane.

We thank Rindy Jaffe for discussions, Allan Jensen for machining work, and Paul McNeil and Rick Steinhardt for useful comments. Preliminary electrophysiological work was done with Jim Galbraith.

This work was partially supported by R01 GM060389-04 to M. Terasaki. The Ti-sapphire microscope was supported by National Institutes of Health 5P41-RR 13186 and 1F10-RR 15705.

Olaf S. Andersen served as editor.

Submitted: 29 March 2005

Accepted: 24 June 2005

REFERENCES

- Bansal, D., K. Miyake, S.S. Vogel, S. Groh, C.C. Chen, R. Williamson, P.L. McNeil, and K.P. Campbell. 2003. Defective membrane repair in dysferlin-deficient muscular dystrophy. *Nature*. 423:168–172.

- Cerny, J., Y. Feng, A. Yu, K. Miyake, B. Borgonovo, J. Klumperman, J. Meldolesi, P.L. McNeil, and T. Kirchhausen. 2004. The small chemical vacuolin-1 inhibits Ca^{2+} -dependent lysosomal exocytosis but not cell resealing. *EMBO Rep.* 5:883–888.
- Chambers, R. 1917. Microdissection studies. I. The visible structure of cell protoplasm and death changes. *Am. J. Physiol.* 43:1–12.
- Chang, D.C., and T.S. Reese. 1990. Changes in membrane structure induced by electroporation as revealed by rapid-freezing electron microscopy. *Biophys. J.* 58:1–12.
- Debska, G., A. Kicinska, J. Skalska, and A. Szewczyk. 2001. Intracellular potassium and chloride channels: an update. *Acta Biochim. Pol.* 48:137–144.
- Demaurex, N. 2002. pH homeostasis of cellular organelles. *News Physiol. Sci.* 17:1–5.
- Detrait, E., C.S. Eddleman, S. Yoo, M. Fukuda, M.P. Nguyen, G.D. Bittner, and H.M. Fishman. 2000a. Axolemmal repair requires proteins that mediate synaptic vesicle fusion. *J. Neurobiol.* 44:382–391.
- Detrait, E.R., S. Yoo, C.S. Eddleman, M. Fukuda, G.D. Bittner, and H.M. Fishman. 2000b. Plasmalemmal repair of severed neurites of PC12 cells requires Ca^{2+} and synaptotagmin. *J. Neurosci. Res.* 62:566–573.
- Eddleman, C.S., G.D. Bittner, and H.M. Fishman. 2000. Barrier permeability at cut axonal ends progressively decreases until an ionic seal is formed. *Biophys. J.* 79:1883–1890.
- Galbraith, J.A., and M. Terasaki. 2003. Controlled damage in thick specimens by multiphoton excitation. *Mol. Biol. Cell.* 14:1808–1817.
- Gillot, I., B. Ciapa, P. Payan, G. De Renzis, G. Nicaise, and C. Sardet. 1989. Quantitative X-ray microanalysis of calcium in sea urchin eggs after quick-freezing and freeze-substitution. Validity of the method. *Histochemistry.* 92:523–529.
- Gunther, W., A. Luchow, F. Cluzeaud, A. Vandewalle, and T.J. Jentsch. 1998. ClC-5, the chloride channel mutated in Dent's disease, colocalizes with the proton pump in endocytotically active kidney cells. *Proc. Natl. Acad. Sci. USA.* 95:8075–8080.
- Hagiwara, S., S. Ozawa, and O. Sand. 1975. Voltage clamp analysis of two inward current mechanisms in the egg cell membrane of a starfish. *J. Gen. Physiol.* 65:617–644.
- Heilbrunn, L.V. 1930. The action of various salts on the first stage of the surface precipitation reaction in arbacia egg protoplasm. *Protoplasma.* 11:558–573.
- Hibino, M., H. Itoh, and K. Kinoshita Jr. 1993. Time courses of cell electroporation as revealed by submicrosecond imaging of transmembrane potential. *Biophys. J.* 64:1789–1800.
- McNeil, P.L., R.F. Murphy, F. Lanni, and D.L. Taylor. 1984. A method for incorporating macromolecules into adherent cells. *J. Cell Biol.* 98:1556–1564.
- McNeil, P.L., and R. Khakee. 1992. Disruptions of muscle fiber plasma membranes. Role in exercise-induced damage. *Am. J. Pathol.* 140:1097–1109.
- McNeil, P.L., and R.A. Steinhardt. 2003. Plasma membrane disruption: repair, prevention, adaptation. *Annu. Rev. Cell Dev. Biol.* 19:697–731.
- McNeil, P.L., S.S. Vogel, K. Miyake, and M. Terasaki. 2000. Patching plasma membrane disruptions with cytoplasmic membrane. *J. Cell Sci.* 113:1891–1902.
- Nilius, B., and G. Droogmans. 2003. Amazing chloride channels: an overview. *Acta Physiol. Scand.* 177:119–147.
- Nuccitelli, R. 2003. A role for endogenous electric fields in wound healing. *Curr. Top. Dev. Biol.* 58:1–26.
- Opresko, L., H.S. Wiley, and R.A. Wallace. 1980. Differential post-endocytotic compartmentation in *Xenopus* oocytes is mediated by a specifically bound ligand. *Cell.* 22:47–57.
- Reddy, A., E.V. Caler, and N.W. Andrews. 2001. Plasma membrane repair is mediated by Ca^{2+} -regulated exocytosis of lysosomes. *Cell.* 106:157–169.
- Shen, S., and R.A. Steinhardt. 1976. An electrophysiological study of the membrane properties of the immature and mature oocyte of the batstar, *Patiria miniata*. *Dev. Biol.* 48:148–162.
- Shen, S.S., W.C. Tucker, E.R. Chapman, and R.A. Steinhardt. 2005. Molecular regulation of membrane resealing in 3T3 fibroblasts. *J. Biol. Chem.* 280:1652–1660.
- Spira, M.E., D. Benbassat, and A. Dormann. 1993. Resealing of the proximal and distal cut ends of transected axons: electrophysiological and ultrastructural analysis. *J. Neurobiol.* 24:300–316.
- Steinhardt, R.A., G. Bi, and J.M. Alderton. 1994. Cell membrane resealing by a vesicular mechanism similar to neurotransmitter release. *Science.* 263:390–393.
- Terasaki, M., and L. Jaffe. 1993. Imaging of the endoplasmic reticulum in living marine eggs. In *Cell Biological Applications of Confocal Microscopy*. Vol. 38. B. Matsumoto, editor. Academic Press, Orlando, FL. 211–220.
- Terasaki, M., K. Miyake, and P.L. McNeil. 1997. Large plasma membrane disruptions are rapidly resealed by Ca^{2+} -dependent vesicle-vesicle fusion events. *J. Cell Biol.* 139:63–74.
- Yu, Q.C., and P.L. McNeil. 1992. Transient disruptions of aortic endothelial cell plasma membranes. *Am. J. Pathol.* 141:1349–1360.